Study of the electrothermal switching effect in bulk glassy semiconductors by a computer simulation method

E. MÁRQUEZ, P. VILLARES, R. JIMÉNEZ-GARAY
Departamento de Física Fundamental, Facultad de Ciencias, Universidad de Cádiz, Apartado 40, Puerto Real (Cádiz), Spain

The electrical switching process in glassy semiconductors has been studied by a computer simulation method. The operation of a switching device has been considered from the standpoint of internal heat generation and the attendant rise in device temperature. A simple model has been chosen for an analysis in which the thermal and electrical parameters are related in a non-linear manner through the exponential dependence of conductivity on temperature. Furthermore, field-dependence effects (space-charge formation) are introduced in order to complete the model, which could be called "electronically assisted" thermal breakdown. The simulated current–voltage relationship exhibits a turnover voltage and conditions of negative differential resistance. To summarize, it is demonstrated that the application of a computer simulation is useful, in order to examine the switching phenomenon.

1. Introduction

Reversible electrical switching effect has been reported in a diverse range of materials, including chalcogenide glassy semiconductors [1–3], organic semiconductors [4], and oxides [5]. There are mainly three models which have been put forward to explain the switching phenomenon. They are the electronic model [6, 7], the thermal model [8–11], and the electrothermal model [12–14]. The electronic model is based on the assumption that the electric fields near both the electron- and the hole-injecting contacts are high, because of the presence of hetero-space charge therein, and that both the electron and hole traps are completely filled near the centre.

In thermal models it is assumed that the electronic phenomena, essential for breakdown, are dependent on the electrical behaviour of the semiconductor bulk and not on the conditions at the electrodes. Electro-thermal models constitute the intermediate group between the two mentioned models. It should be emphasized that there is still some controversy [15, 16] about which model can give an adequate description of the switching mechanism.

So far, a great part of the work on switching phenomena has been concentrated on thin films. In this paper, the switching phenomenon in bulk samples is analysed, trying to explain the switching properties in a sandwich-type switching device, designed and built in our laboratory [17].

2. Description of the model

In all cases reported so far, switching phenomenon in chalcogenide glasses is associated, either explicitly or implicitly, with a region of current-controlled negative resistance (CCNR). An essential condition for CCNR is a positive feedback mechanism, which, in the region

of instability, allows the system to carry the same or even larger currents with smaller applied voltages. In the thermal mechanisms of switching, we assume that the feedback loop is that shown in Fig. 1. The essential link is the sensitivity of conductivity to temperature.

As in any thermal breakdown, the fundamental expression is the heat equation

$$C_v \frac{\partial T}{\partial t} = \text{div} (k \text{ grad } T) + \sigma E^2 \qquad (1)$$

where k and σ are the glass thermal and electrical conductivities, respectively, and C_v is the specific heat per unit volume. Furthermore, as we shall deal only with cases of no charge accumulation, the equation of current continuity is $\text{div}(\sigma E) = 0$. If the result is breakdown, the conditions leading to the electrical instability can usually be formally described by an equation as [18]

$$A(T, E, \alpha) = B(T, \alpha) \qquad (2)$$

where A is the rate at which the energy is increased by the field E at temperature T, and B is the rate at which it is dissipated. The parameter α is introduced to denote any other relevant property of current carriers due to a particular situation. The simplest form of thermal breakdown occurs when $\sigma = \sigma(T)$ [19]. In higher resistivity glasses, the dependence of conductivity on field is more important, i.e. $\sigma = \sigma(T, E)$. When this occurs, the process can be called "electronically assisted" thermal breakdown.

The aim of this work is the computer simulation of reversible electrical switching phenomenon, first based on a simple model of basically thermal nature, and later, including electronic effects (due to high fields), that produce a non-ohmic conduction. The application of this model is restricted to bulk samples, where
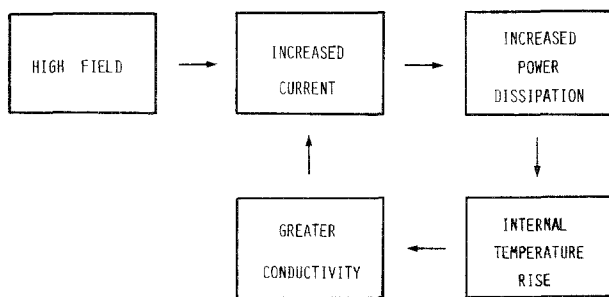
Figure 1 Positive feedback loop corresponding to a thermal nature mechanism for switching.

this kind of mechanism can take place, according to experimental evidence [17]. According to Rycerz [7], the electronic nature mechanisms arising in high fields can mainly account for the switching behaviour in thin films.

This study is based on two programs, A and B. The first simulates the process originated when a constant voltage is applied, and the second one, the process originated by a constant current. The results obtained by the simulation were contrasted with the experimental ones, in order to verify the validity of the model.

The device geometry is shown in Fig. 2, where different parts of switching device appear. The essential features are: (i) its sandwich electrode configuration and (ii) the isolating layer covering the device. The electrode material is copper and the good electrodes–glassy material electrical contact is reached using silver paste. This device offers experimentally stable reproducible switching characteristics. The semiconducting glass is approximately 1.0 mm thick and it is inlaid in epoxy-type resin, so that the heat flows away fundamentally in the electrodes (though it is limited by the isolator). Therefore, heat flow is nearly parallel to current flow. Experimental results mentioned in this work are from an active material with a composition $As_{0.40}Se_{0.30}Te_{0.30}$, that is, a typical chalcogenide glassy semiconductor.

From Equation 1, and assuming that temperature is approximately the same for electrodes and active material, the resulting equation is

$$C\frac{dT}{dt} = VI - K_{th}(T - T_a) \qquad (3)$$

where $V = IR(T)$; and C is the specific heat of device, I the current, V the applied voltage, T_a the ambient
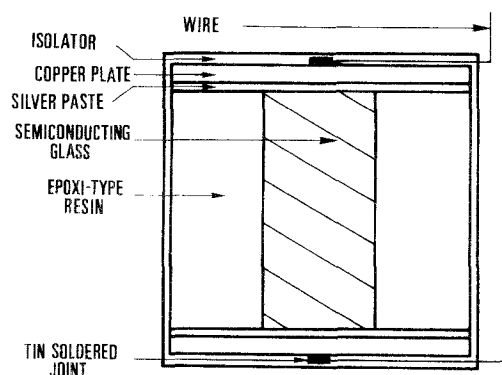

Figure 2 Bulk sample-based sandwich device.

temperature, $R(T)$ the electrical resistance, and K_{th} the device thermal conductance. The use of Equation 3 is justified because the heat evacuation controlling device elements, are the isolating layers covering the electrodes. It is assumed that the difference in temperature occurs between the ambient around the device and electrodes which, as pointed out, are supposed to be at the same temperature as the glass material. The electrical resistance obeys the equation ("intrinsic"-type behaviour)

$$R(T) = R_a \exp\left[\left(\frac{\Delta E}{k_B}\right)\left(\frac{1}{T} - \frac{1}{T_a}\right)\right] \qquad (4)$$

where R_a is the electrical resistance at ambient temperature, ΔE the activation energy, and k_B the Boltzmann constant.

From Equations 3 and 4

$$dT = \frac{1}{C}\left[\left(\frac{V^2}{R_a}\right)\exp\left[\left(\frac{\Delta E}{k_B}\right)\left(\frac{1}{T_a} - \frac{1}{T}\right)\right]\right.$$
$$\left. -K_{th}(T - T_a)\right]dt$$
$$= F_1(T; V)dt \qquad (5)$$

The expression is valid when a constant voltage is applied to the device, and it allows the simple evaluation by consecutive integrations of time evolution of temperature during the electrical excitation. To do this, Equation 5 becomes

$$t(T) = \int_{T_a}^{T}\frac{dT}{F_1(T; V)} \qquad (6)$$

This integral cannot be determined analytically, and therefore, it has been solved by numerical methods (Simpson's rule).

Program A consists, essentially, in solving consecutively the integral in Equation 6, for increasing upper limits. The value of temperature increase, ΔT, in each step is adjusted conveniently in agreement with the process stage in which it is placed. So, initially the temperature is increased by $1°C$ and, if the resulting time differs substantially from the previous one, the increase is reduced to $0.5°C$, starting the numerical integration again. So, consecutively, the temperature increase is divided by two, until it reaches an instant, whose difference with the previous one, is lower than an initially established maximum period of time, Δt_{max}. Its value in the present case was 0.1 sec. This is an appropriate value, because delay times obtained by simulation are much higher than the chosen maximum time increase Δt_{max}. This permits us to obtain a complete characterization of time evolution of temperature. The interval of temperature determined by limits of integral (T_a, T) is divided, when the numerical integration is carried out, in a suitable number of subintervals in order to obtain a negligible integration error. If the number of subintervals is n, the committed error using Simpson's rule is $[(T - T_a)/n]^5$.

In every step of the simulation process carried out with program A, resistance and current are determined in such a way that their dependences on time are known. When the process is simulated, two physical

situations can appear: an equilibrium or steady state situation can be reached or switching can occur. To detect the first situation, the program uses a minimum value $(\Delta T/\Delta t)_{min}$, and the second one is detected by using a maximum value $(\Delta T/\Delta t)_{max}$, both of them directed to control the temperature rise in each step of the simulation process. Therefore, through program A, voltage–delay time (t_D) characteristics can be found, allowing us to obtain, by extrapolation, the corresponding voltage at $t_D = \infty$; i.e. the lowest voltage to generate the transition from OFF to ON-state, called threshold voltage. Using the mentioned method, the positive feedback loop, shown schematically in Fig. 1, is generated. Furthermore, the program permits determination of the time dependence of dT/dt, clarifying the possible process of crystallization that causes the memory phenomenon, because the heating rate has a notable influence on nucleation and crystalline growth [20, 21].

Program B allows the simulation of the process of reaching thermally induced negative differential resistance. Furthermore, it is possible to determine the turnover voltage and the corresponding current, as well as the influence of activation energy in the CCNR region. The loop in this case is the following: a constant current is carried through the device, generating Joule heating in the material, which produces a decrease in electrical resistance. Thus the voltage across the sample decreases. In this program, the detection of the equilibrium situation is made as before, through a minimum value, in such a way that, if after each step, $\Delta T/\Delta t$ is lower than the established value, the simulation is stopped. The expression used in this program to determine the basic algorithm is

$$dT = \frac{1}{C}\left[I^2 R_a \exp\left[\left(\frac{\Delta E}{k_B}\right)\left(\frac{1}{T} - \frac{1}{T_a}\right)\right] \right.$$
$$\left. - K_{th}(T - T_a) \right] dt$$
$$= F_2(T; I)\, dt \qquad (7)$$

As in the other program, the interval of temperature corresponding to integration limits was divided in an appropriate number of subintervals, so that error is sensibly low. On the other hand, the integral upper limit is increased following a similar procedure as in program A.

3. Results and discussion

Values of parameters used in the process studied are: $\Delta E = 0.5\,\text{eV}$, $T_a = 55°\text{C}$ (because experimental results to be contrasted with those obtained by simulation were determined at this temperature), $R_a = 9.1\,\text{M}\Omega$ and $K_{th} = 0.9\,\text{mW K}^{-1}$ (this parameter has been determined experimentally, analysing the steady-state I–V characteristics, and using the usual Newton expression $VI = K_{th}\Delta T$). Specific heat has been determined by means of device volume (approximately $10\,\text{mm}^3$) and specific heat per unit volume, whose value in this kind of material is about $2 \times 10^6\,\text{J m}^{-3}\text{K}^{-1}$ [8]. The value of specific heat was found to be $2 \times 10^{-2}\,\text{J K}^{-1}$.
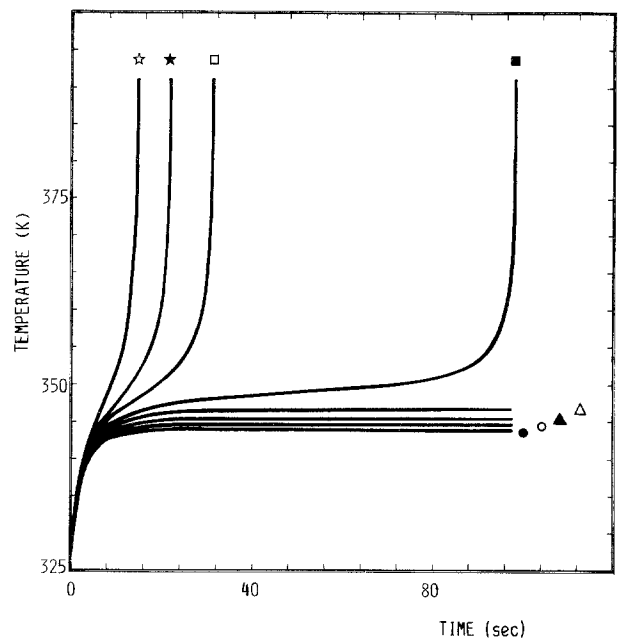
Figure 3 The time dependence of the temperature during the electrical stimulation. (☆) 252 V, (★) 248 V, (□) 246 V, (■) 244 V, (△) 243 V, (▲) 242 V, (○) 241 V, (●) 240 V.

Fig. 3 shows the results of program A. Eight curves are plotted, pointing out the time evolution of material temperature at the indicated voltages. It is observed that the first voltage to reach electrical switching is 244 V (the corresponding delay time is 97.6 sec), and differences between delay time values decrease as voltages increase. From delay time experimental values, corresponding to the different applied voltages, and by extrapolating from the V against $1/(t_D)^{1/2}$ plot, a threshold voltage of 264 V was obtained (the percentage deviation between experimental and simulated values is lower than 8%).

Another point to observe is that the overall speed for the entire process is very fast, considering the thermal nature of the model. It is then interesting to note that comparatively long times are required for increasing the device temperature to threshold levels, but the subsequent temperature increase can occur at an exceedingly high rate. This is the reason why this process may be described as one of thermal avalanche [19].

From Fig. 3 it is deduced that the highest voltage that originates a stable situation is 243 V, associated with a temperature increase of 18.5 K. This value coincides with the critical increase in temperature corresponding to the turnover point (zero differential resistance), anticipated by thermistor-type behaviour, which is expressed as approximately $k_B T_a^2/\Delta E$ [14].

Program A has also considered the dependence of isothermal resistance on voltage appearing when the electronic effects are introduced. Electrical resistance considering non-ohmic effects, is expressed by [2, 12, 17]

$$R(V; T_a) = R_{a,ohm} \exp\left(-\frac{V}{V_0}\right) \qquad (8)$$

where V_0 is a parameter whose value is $\sim 10^3$ V for the studied glassy alloy, and indicates the voltage range over which electronic effects become significant. So,
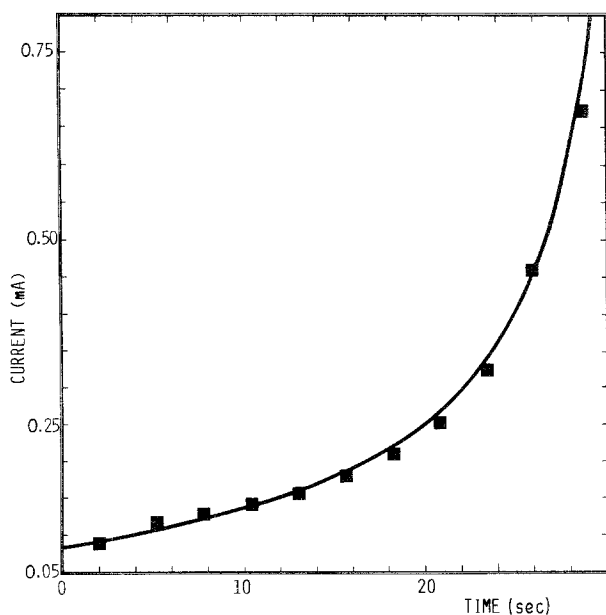
Figure 4 The time dependence of the current obtained by the simulation (——), with the experimental values (■). SCLC effects, $R = R_a \exp(-V/V_0)$.

Figure 5 Current–steady state voltage characteristics at the ambient temperature of 55° C.

program A also permits a phenomenon simulation, considering its possible electrothermal nature, i.e. an electronic contribution may be included. The functional dependence 8 points out that, in the pre-switching region, current flow is space-charge limited (SCLC), and the Fermi level is in a uniform distribution of traps [22]. In this mechanism of electronic conduction in the OFF-state, the expression of the parameter V_0 is

$$V_0 = \frac{eN_t k_B T d^2}{\varepsilon} \qquad (9)$$

where ε is the dielectric constant, N_t is the trap density, and d is the device thickness. In the present case, the value of d is 1.0 mm and that of ε is 17.7 (in cgs units) [17], from where it is deduced that the trap density is $\sim 10^{14} \mathrm{cm}^{-3} \mathrm{eV}^{-1}$.

In Fig. 4, current is shown plotted against time, obtained from simulation values with SCLC electronic effects consideration. As can be seen, a good agreement is observed between experimental and simulated values for the same voltage ($V = 400\,$V and $t_D = 284\,$sec) and temperature. In Table I, turn-on times obtained by simulation and corresponding to different voltages and at the same temperature, appear. As in the case of the voltage of 400 V, results of delay

TABLE I Variation of delay time with applied voltage obtained by simulation. The ambient temperature was 55° C

Applied voltage (V)	Turn-on time (sec)
350	59.8
360	46.3
370	41.1
380	34.3
390	29.6
400	25.0
410	21.8
420	19.2
430	16.6
440	14.0

time measurements, corresponding to the rest of voltages considered in simulation, are similar to those shown in Table I. Therefore, results from program A indicate a good agreement between the simulation and experimental data, pointing out that the inherent mechanism of the electrothermal model can be the fundamental reason for the phenomenon. The principal objection for applying the thermal model to switching devices has been allegedly high speed. Nevertheless, through this simulation it has been shown that the high transition speed could possibly be consistent with the electrothermal mechanism.

Results corresponding to program B are shown in Fig. 5, where characteristic current-controlled negative differential resistance region appears. The turnover current is about $80\,\mu$A and the turnover voltage 244 V, in agreement with the lowest voltage to generate the switching obtained by program A. This verifies the model coherence, because the maximum electric power dissipated by the device, without thermal instability, is $P_{th} = K_{th}(k_B T_a^2/\Delta E) = 16.7\,$mW, and in both programs the result is near this value. In program A, for a voltage of 244 V, a steady state current near $80\,\mu$A is obtained, whilst in program B, using a similar current value, approximately the same steady state voltage value is obtained.

It can be concluded that the CCNR region and the substantial negative temperature coefficient of electrical resistance, are those characterizing a thermistor-type device. The analysis discussed in this work also justifies the use of the computer simulation of electrical switching effects, as a tool for the design of electronic devices.

Acknowledgements

References

1. S. R. OVSHINSKY, *Phys. Rev. Lett.* **21** (1968) 1450.
2. E. MÁRQUEZ, P. VILLARES and R. JIMÉNEZ-GARAY, *J. Non-Crystalline Solids* **74** (1985) 195.

3. J. VÁZQUEZ, E. MÁRQUEZ, P. VILLARES and R. JIMÉNEZ-GARAY, *Mater. Lett.* **4** (1986) 360.
4. H. CARCHANO, R. LACOSTE and Y. SEGUI, *Appl. Phys. Lett.* **19** (1971) 414.
5. C. F. DRAKE, I. F. SEANLAN and A. ENGEL, *Phys. Status Solidi* **32** (1969) 193.
6. H. FRITZSCHE and S. R. OVSHINSKY, *J. Non-Crystalline Solids* **2** (1970) 538.
7. Z. RYCERZ, *Comput. Phys. Commun.* **15** (1978) 15.
8. A. C. WARREN, *J. Non-Crystalline Solids* **4** (1970) 613.
9. A. ALEGRÍA, A. ARRUABARRENA and F. SANZ, *ibid.* **58** (1983) 17.
10. M. M. HAIFZ, M. M. IBRAHIM, M. DONGOL and F. M. HAMMAD, *J. Appl. Phys.* **54** (1983) 1950.
11. J. TRÖLTZSCH and CH. DIPPMANN, *Phys. Status Solidi* **67** (1981) 527.
12. E. MÁRQUEZ, P. VILLARES and R. JIMÉNEZ-GARAY, *Mater. Lett.* **4** (1986) 52.
13. K. NAKASHIMA and K. C. KAO, *J. Non-Crystalline Solids* **33** (1979) 189.
14. A. E. OWEN, J. M. ROBERTSON and C. MAIN. *ibid.* **32** (1979) 29.
15. N. F. MOTT, *Philos. Mag.* **32** (1975) 159.
16. T. MIYAZONO, Y. AKIBA and M. IIDA, *Jpn J. Appl. Phys.* **14** (1975) 969.
17. E. MÁRQUEZ, MSc thesis, Seville University (1986).
18. J. J. O'DYWER, "The Theory of Dielectric Breakdown of Solids" (Oxford University Press, Oxford, 1964).
19. F. M. COLLINS, *J. Non-Crystalline Solids* **2** (1970) 496.
20. E. MÁRQUEZ, P. VILLARES and R. JIMÉNEZ-GARAY, *Mater. Lett.* **3** (1985) 503.
21. M. HARO, E. MÁRQUEZ, L. ESQUIVIAS and R. JIMÉNEZ-GARAY, *J. Non-Crystalline Solids* **81** (1986) 255.
22. A. E. OWEN and J. M. ROBERTSON, *IEEE Trans. Electron Devices* **20** (1973) 105.